İSTANBUL UNIVERSITY PRESS

Texture Analysis of Thyroid Nodules Using Computed Tomography: Is it a Viable Method for Objective Assessment of Thyroid Nodules?

Sefa İncaz[1] , Ömer Tarık Kavak[2] , Burak Kersin[3] , Ali Cemal Yumuşakhuylu[2]

[1]Medient, Ear Nose and Throat Medical Center, İstanbul, Türkiye
[2]Marmara University Faculty of Medicine, Pendik Training and Research Hospital, Department of Otorhinolaryngology, İstanbul, Türkiye
[3]İstanbul Kartal Dr. Lütfi Kırdar City Hospital, Department of Otorhinolaryngology, İstanbul, Türkiye

ORCID ID: S.İ. 0000-0002-1937-215X; Ö.T.K. 0000-0003-2603-3866; B.K. 0000-0002-9644-4583; A.C.Y. 0000-0002-8421-211X

ABSTRACT

Objective: Computed aided detection (CAD) systems can be developed to help radiologists in the accurate interpretation of computed tomography (CT) images. The recently popularised texture analysis method allows for qualitative and quantitative evaluation by analysing the grey-level distribution and relationships within an image. We aimed to compare the ratios of texture analysis data in the differentiation of benign-malignant nodules with the proportions of radiologists in the distinction between benign and malignant nodules and to compare the results.

Materials and Methods: Retrospectively, the data of 80 patients who underwent thyroidectomy and had contrast-enhanced neck CT preoperatively were analysed. Two radiologists, experienced in head and neck radiology, blinded to the patients' data evaluated neck CT images. Manual marking was performed and scanned to take tissue sections from the nodule area in transverse contrast-enhanced CT images, and the size of the nodule in the contralateral normal thyroid parenchyma was almost equal.

Results: The computed tomography texture analysis (CTTA) model achieved the highest sensitivity of 81.4%, followed by the first radiologist at 51.2% and the second radiologist at 55.8%. Additionally, the CTTA model achieved the highest accuracy at 61.3%, followed by the first radiologist at 41.3% and second radiologist at 47.5%. On average, the CTTA model performed significantly better than the two radiologists, especially with regard to sensitivity.

Conclusion: The CTTA model was superior to both radiologists in differentiating between benign and malignant thyroid nodules. Medical experts can benefit from CTTA-based solutions to extend their understanding of thyroid nodules in their routine practise.

Keywords: Texture analysis, thyroid cancer, computer-aided diagnosis, thyroid nodules

INTRODUCTION

Thyroid carcinomas account for 2,5% of all cancers and 95% of all endocrine tumours (1). Most thyroid carcinomas are differentiated tumours with a slow progression (2). Although ultrasound examination reveals thyroid nodules in up to 70% of adults, only <7% of these nodules are diagnosed as malignant (3). To avoid unnecessary surgical interventions, the differential diagnosis of malignant or benign nodules should be performed precisely. Fine needle aspiration biopsy (FNAB) and noninvasive imaging techniques are the basic approaches and equipment that enable us to differentiate between malignant and benign nodules. Ultrasonography (USG) is an accurate and efficient diagnostic tool for the detection of thyroid nodules and differentiation between malignant and benign nodules (4). Due to its high specificity and sensitivity, noninvasiveness, and low cost, USG is the first test requested when a patient presents with suspicion of a thyroid nodule. The characteristics of thyroid nodules on USG, such as hypoechogenicity, irregular margins, solid component, microcalcifications, and taller-than-wide shape, can show a significant relationship with malignant nodules (4). For many thyroid nodules, USG and FNAB are quite effective and sufficient for decision making. There are a substantial number of patients with no obvious suspicion of malignancy on thyroid USG and whose FNAB was reported as undetermined cytology (Bethesda 3 or 4). It is known that

Follicular Thyroid Cancer (FTC) and Follicular-variant of Papillary Thyroid Cancer (FVPTC) display relatively benign sonographic features in contrast to conventional variants of papillary thyroid carcinoma (5, 6). In this group of patients, in addition to USG and FNAB, other imaging modalities may impact the decision-making process.

Computed Tomography (CT) is not initially used to evaluate thyroid nodules; however, it provides valuable information in some circumstances, such as retrosternal goitres, malignant tumours with extrathyroidal extension, or lymph node metastasis, and also in the follow-up of thyroid cancer, especially in cases of suspected structural disease recurrence (7, 8). In clinical practise, radiologists visually inspect a large number of CT images, and some subtle CT features, like calcification, could be missed during visual inspection. In a retrospective study by Saaedan et al., it was reported that 48% of patients with intrathyroidal calcification were diagnosed with thyroid carcinoma by histopathology, and increased rates of thyroid cancer and lymph node metastasis were observed in patients with calcified nodules (9). Computed aided detection (CAD) systems can be developed to help radiologists in the accurate interpretation of CT images.

The recently popularised texture analysis method allows for qualitative and quantitative evaluation by analysing the grey-level distribution and relationships within an image. Because of the possible heterogeneous structure of the tumour tissue, the texture analysis procedure can give varying results. Typically, medical images contain an extensive amount of tissue information. For instance, CT or MR images cannot provide microscopic details that can be visually evaluated; however, histological changes caused by certain diseases may cause tissue changes that can be quantified on CT and MR images. In other words, while the information obtained from CT or MR images is limited regarding the nature of the tissue, the quantitative data obtained from texture analysis has increased our understanding of histological changes and possible diseases (10).

The objective of our study was to investigate the differences in tissue analysis parameters obtained from CT images between malignant and benign nodules and to evaluate the potential clinical utility of these differences in distinguishing between malignant and benign nodules. In addition, we aimed to compare the ratios of texture analysis data in the differentiation of benign-malignant nodules with the proportions of radiologists in the distinction between benign and malignant nodules and to compare the results obtained with those found in the literature.

MATERIALS and METHODS

Patients

The Marmara University Faculty of Medicine Ethics Committee for Clinical Research approved the study on June 18, 2021, with the number 09.2021.396. Informed consent was not obtained from patients because of the retrospective design of the study. Retrospectively, the data of 525 patients who underwent thyroidectomy surgery between January 2012 and April 2021 were analysed through the hospital automation system. Neck CT was performed in 150 of these 525 patients for any reason (retrosternal extension, suspicion of extrathyroidal invasion or lymphatic spread in malignant cases, and any suspected neck pathology independent of the thyroid), and in 80 of them, images that were demarcation of the borders of the nodules apparent and contrast-enhanced were included in the study (Figure 1).

Computed tomography acquisition and image review

Contrast-enhanced neck CT scans of the patients were performed in the supine position, the neck in the extended position as much as possible, the scanning range from the oropharynx to the supraclavicular region, with the Philips Brilliance ICT 256 device with intravenous contrast, with the technical parameters specified. The tube potential is 100-120kVp, tube current is 200 mAs, cross-section gap is 3.75 mm, section thickness is 3 mm, field of view (FOV) values are 250 mm, and pitch is 0.1. In CT scans, 80-100 ml of nonionic iodinated contrast material (Omnipaque 300, 300 mg I/mL; Amersham Health, Cork, Ireland) was administered via the antecubital vein in an amount of 1.2 mL/kg and at a rate of 2-3 mL/s. The scan delay was 40-50 seconds.
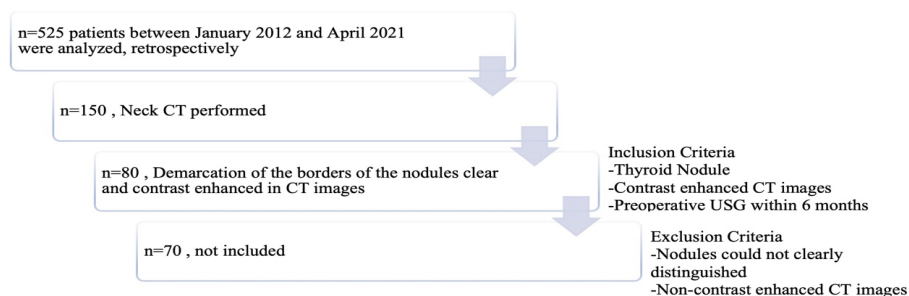
Figure 1: Patient selection flowchart following the application of inclusion and exclusion criteria.

Computed tomography texture analysis (CTTA)

Two radiologists, experienced in head and neck radiology, blinded to the patients' clinical information, preoperative examinations, or postoperative histopathological diagnoses evaluated neck CT images. The most prominent and suspicious nodule on USG was found and determined on contrast-enhanced neck CT of the patients. Manual marking was performed and scanned to take tissue sections from the nodule area in transverse contrast-enhanced CT images, and the size of the nodule was almost equal to that of the contralateral normal thyroid parenchyma (Figure 2). Sections and markings were made in the same way for each patient. A total of 160 (80 nodule area, 80 contralateral nodule-free area) images were obtained. Texture analysis measurements were made from pictures taken separately from both sides (with and without nodules). Texture analysis and histogram evaluations were performed using the MaZda programme (MaZda 4.60, The Technical University of Lodz, Institute of Electronics, Poland). To evaluate tissue properties, 21 parameters were examined, including the Hounsfield Unit (HU) value.
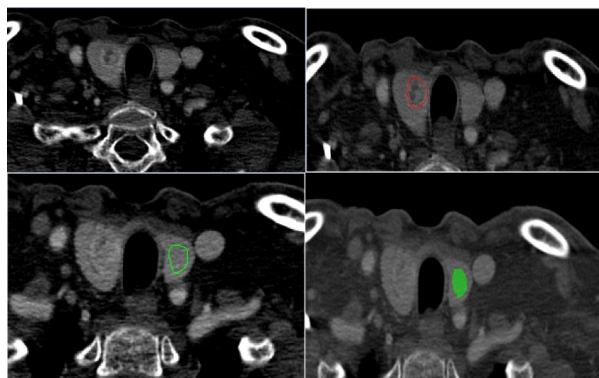
Figure 2: Manuel marking of the nodule and nodule-free area.

The following four stages were carried out in the study:

1-Based on the postoperative thyroid histopathology results, patients were divided into benign and malignant groups. A comparison was made between the preoperative USG findings and texture analysis measurements obtained from the nodule location.

2-Tissue analysis measurements taken from the nodule area were compared between the two groups.

3- The texture analysis measurements obtained from the nodule area of patients in the benign and malignant groups and those obtained from the contralateral nodule-free site (with normal thyroid parenchyma) were compared.

4-To investigate the views of clinical experts in radiology regarding the prediction of thyroid nodules as benign or malignant and compare texture analysis data with the results.

Statistical analysis

SPSS 22 (IBM SPSS Corp., Armonk, NY, USA) programme was used in the analysis of the data. Data are presented as numbers, percentages, mean, standard deviation, and median. The Kolmogorov–Smirnov test was used for the normality test. Parametric analyses were preferred in the study of normally distributed data, and non-parametric analyses were preferred in non-normally distributed data analysis. The analysis used the Mann–Whitney U, Kruskal–Wallis, and Spearman correlation tests. A value of $p<0.05$ was considered statistically significant.

RESULTS

Table 1 presents the demographic details of the patients and the preoperative USG features of the thyroid nodules.

Table 1: Demographics of patients and preoperative USG characteristics of thyroid nodules

	Bening n=37	Malignant n=43
Mean Age 52.00±17.05 (min=11-max=78). 32.5% (n:26) **male** / 67.5% (n:54) **female**		
Number of patients (n = 80)	37 (46.25%)	43 (53.75%)
Extent of the Surgery		
Total thyroidectomy	32 (40%)	43 (53.75%)
Lobeisthmectomy	5 (6.25%)	0
Neck dissection	0	16 (20%)
Preoperative USG Findings		
Calcification (n = 26) (32.5%)	8 (10%)	18 (22.5%)
Microcalcification (n = 14)	0	14
Echogenicity		
Hypoechoic (n=39) (48.8%)	10 (12.5%)	29 (36.25%)
Isoechoic (n=13) (16.3%)	6	7
Hyperechoic (n=2) (2.5%)	2	0
No evaluation (n=26) (32.4%)		
Solid/Cystic Characteristic		
Solid (n=39) (48.8%)	14 (17.5%)	25 (35%)
Cystic (n=11) (13.8%)	9 (11.25%)	2 (2.5%)
Mixed (n=8) (10%)	2 (2.5%)	6 (7.5%)
No evaluation (n=22) (27.4%)		

The percentages in parentheses are calculated based on the total number of patients (n=80).

Comparative analysis of preoperative USG and CTTA measurements

This study revealed a statistically significant disparity in the correlation (Correlat) values obtained from CTTA measurements based on calcification within the tissue. Notably, individuals with calcification exhibited a higher correlation (Correlat) value, as shown in Table 2.

Upon comparing CT measurements based on the solid and cystic structure of the nodule, a statistically significant difference was observed in the mean (Mean), kurtosis (Kurtosis), histogram panels (Perc01, Perc10, Perc50, Perc90, Perc99), and HU values (Table 3). The post hoc analysis of the measurements revealed

Table 2: Comparison of CT texture analysis based on the presence or absence/not evaluated of calcification in USG

| | CALCIFICATION | | | | | | |
| | Present | | | Absence/Not evaluated | | | |
	X	SD	Median	X	SD	Median	p
Mean	1134.14	38.02	1134.29	1122.35	40.31	1123.19	0.312
Variance	1618.70	1764.36	954.89	2341.99	6171.39	1116.42	0.801
Skewness	-0.11	2.34	0.01	0.25	2.38	0.05	0.825
Kurtosis	8.27	36.00	0.14	10.15	33.10	0.07	0.865
Perc01	1064.85	44.70	1063.00	1048.30	43.39	1044.50	0.237
Perc 10	1091.88	41.36	1085.50	1078.61	41.18	1074.50	0.358
Perc50	1133.58	37.71	1134.50	1120.72	40.30	1121.50	0.256
Perc90	1175.31	44.43	1173.00	1166.56	50.57	1161.00	0.281
Perc99	1226.19	96.63	1206.00	1221.83	145.07	1186.50	0.369
AngScMom	0.00	0.00	0.00	0.00	0.00	0.00	0.438
Contrast	77.88	37.42	74.56	99.46	45.82	91.41	0.057
Correlat	**0.61**	**0.18**	**0.66**	**0.51**	**0.20**	**0.49**	**0.027**
SumOfSqs	100.41	14.33	105.43	99.73	17.35	105.70	0.988
InvDfMom	0.18	0.07	0.16	0.16	0.06	0.14	0.082
SumAverg	64.14	1.24	64.33	64.13	1.18	64.32	0.662
Sum Varnc	323.78	59.30	333.70	299.46	63.71	299.96	0.106
SumEntrp	1.79	0.08	1.81	1.78	0.11	1.82	0.922
Entropy	2.75	0.25	2.83	2.77	0.28	2.85	0.569
DifVarnc	31.25	13.35	30.28	38.11	16.44	41.55	0.089
DifEntrp	1.19	0.12	1.22	1.24	0.13	1.26	0.082
HU	117.33	39.74	114.58	108.27	39.04	107.72	0.337

P values that are statistically significant and their related row are highlighted in bold. X: Mean value, SD: Standard deviation; HU: Hounsfield Unit

Table 3: Comparison of CT texture analysis based on solid or cystic characteristics as observed by ultrasound

| | SOLID-CYSTIC | | | | | | | | | | | | |
| | Solid | | | Cystic | | | Solid+Cystic | | | No evaluation | | | |
	X	SD	Median	X	SD	Median	X	SD	Median	X	SD	Media	p
Mean	1140.94	31.26	1135.00	1106.85	38.87	1126.15	1144.80	47.43	1147.58	1102.92	37.43	1102.58	0.002
Variance	2697.24	7187.58	1104.28	1296.69	784.73	897.26	3317.95	3163.37	2123.69	1025.21	615.18	938.14	0.523
Skewness	-0.34	2.72	-0.02	0.65	1.57	0.39	2.27	3.35	1.48	-0.06	0.48	0.03	0.054
Kurtosis	14.21	43.36	0.17	5.23	14.82	-0.16	18.96	43.29	3.38	-0.02	0.52	-0.17	0.016
Perc01	1065.51	40.68	1064.00	1033.36	52.59	1030.00	1072.63	33.05	1064.00	1035.95	41.74	1026.50	0.013
Perc10	1096.36	35.80	1096.00	1063.91	47.04	1074.00	1099.25	39.83	1093.50	1062.68	38.83	1056.00	0.006
Perc50	1139.03	31.63	1136.00	1106.64	39.93	1125.00	1139.13	48.72	1139.50	1103.82	38.48	1102.00	0.006
Perc90	1186.10	46.21	1188.00	1149.55	35.12	1147.00	1190.13	57.94	1200.00	1142.18	40.41	1146.50	0.002
Perc99	1242.72	158.90	1207.00	1190.82	38.07	1186.00	1319.38	155.37	1319.00	1170.00	45.56	1171.50	0.006
AngScMom	0.00	0.00	0.00	0.00	0.00	0.00	0.00	0.00	0.00	0.00	0.00	0.00	0.273
Contrast	88.74	37.92	83.30	81.49	42.53	61.81	92.75	54.09	100.84	104.39	51.74	117.03	0.540
Correlat	0.56	0.18	0.60	0.58	0.22	0.70	0.50	0.19	0.49	0.51	0.24	0.47	0.728
SumOfSqs	98.94	17.07	105.37	99.85	14.40	102.87	87.72	27.85	95.90	106.24	4.42	108.53	0.093
InvDfMom	0.17	0.06	0.15	0.17	0.04	0.16	0.22	0.12	0.16	0.15	0.05	0.12	0.293

SumAverg	64.32	1.24	64.45	63.95	1.04	64.30	63.75	1.47	64.03	64.03	1.10	64.32	0.598
SumVame	307.02	61.44	320.48	317.92	73.83	349.54	258.13	74.91	282.27	320.59	49.62	313.46	0.167
SumEntrp	1.78	0.11	1.83	1.79	0.10	1.83	1.72	0.12	1.73	1.81	0.06	1.82	0.133
Entropy	2.75	0.29	2.83	2.76	0.24	2.82	2.65	0.31	2.58	2.84	0.24	2.90	0.405
DifVarne	34.64	13.83	31.38	32.33	17.12	28.01	39.85	17.54	43.09	38.42	17.98	42.86	0.631
DifEntrp	1.21	0.13	1.23	1.21	0.10	1.18	1.18	0.21	1.24	1.26	0.13	1.30	0.354
HU	**127.61**	**32.30**	**137.05**	**98.07**	**33.52**	**107.31**	**121.32**	**47.93**	**120.42**	**85.05**	**35.51**	**82.59**	**<0.001**

P values that are statistically significant and their related row are highlighted in bold. X: Mean value; SD: Standard deviation; HU: Hounsfield Unit

Table 4: Ratio of CT texture analysis values obtained from nodule- and nodule-free regions in both benign and malignant groups.

	DIAGNOSIS						
	Benign			Malign			
	X	SD	Median	X	SD	Median	p
Mean ratio	0.96	0.05	0.96	0.94	0.04	0.94	0.085
Variance ratio	15.52	26.53	3.15	6.78	8.88	4.17	0.253
Skewness ratio	-7.84	74.40	0.19	-0.26	16.23	0.18	0.769
Kurtozis ratio	-138.13	872.55	-0.93	-5.90	54.19	0.03	0.058
perc01 ratio	0.93	0.05	0.92	0.92	0.05	0.92	0.572
perc10 ratio	0.94	0.05	0.93	0.93	0.05	0.93	0.466
perc50 ratio	0.95	0.05	0.96	0.94	0.04	0.94	0.144
perc90 ratio	**0.98**	**0.06**	**0.99**	**0.95**	**0.04**	**0.96**	**0.044**
perc99 ratio	**1.03**	**0.15**	**1.00**	**0.97**	**0.04**	**0.96**	**0.042**
AngScMom ratio	**1.03**	**0.94**	**0.67**	**0.63**	**0.44**	**0.50**	**0.022**
Contrast ratio	0.74	0.58	0.58	1.04	1.36	0.68	0.377
correlate ratio	8.54	38.46	1.74	2.45	1.90	1.80	0.904
SumOfSqs_ratio	0.95	0.21	0.98	1.28	1.62	0.99	0.566
InvDfMom ratio	1.60	0.81	1.37	1.38	0.60	1.28	0.347
SumAverg_ratio	0.99	0.02	1.00	0.99	0.03	0.99	0.889
SumVarnc ratio	1.12	0.31	1.09	1.49	1.82	1.12	0.612
SumEntrp_ratio	1.03	0.09	1.03	1.07	0.09	1.06	0.052
Entropy ratio	**1.08**	**0.14**	**1.08**	**1.15**	**0.13**	**1.15**	**0.023**
DifVarne ratio	0.81	0.57	0.72	1.12	1.44	0.77	0.599
DifEntrp ratio	0.92	0.12	0.93	0.97	0.17	0.96	0.185

P values that are statistically significant and their related row highlighted in bold
X: Mean value; SD: Standard deviation

that the statistical disparity was attributable to the solid and unevaluated groups.

Comparative analysis of postoperative histopathology and CTTA measurements

The study involved categorising patients into two distinct groups based on the nature of their condition: benign and malignant. CTTA values obtained from nodule sections of both groups were compared. No statistically significant difference was observed when comparing CTTA measurements between benign and malignant nodules.

The logistic regression model established the significance of incorporating texture analysis measurements of the CT section where the nodule is situated in estimating nodules' benign-malignant risk (p=0.021). The model's dependent variable pertains to the pathology result of the nodule, specifically whether it is benign or malignant. The model's independent variables consist of CTTA values obtained from the nodule region. The model's accuracy rate is 61.3%. The independent variables account for 19.2% of the variability observed in the dependent variable. The Forward LR method was employed as the primary modelling technique. The utilisation of Histogram

percentage-99% (Perc99) and HU measurements substantially contributes to the model. The study revealed that an elevation in the Perc99 measurement by 0.006 units results in a 1.006-fold decrease in the likelihood of malignancy. Conversely, an increase in the HU measurement by 0.023 units results in a 1.024-fold increase in the risk of malignancy.

Comparative analysis of CTTA measurements of nodule and nodule-free areas

Table 4 compares the ratios of CTTA values obtained from the thyroid nodule and CTTA analysis measurements taken from the side opposite to the nodule (nodule-free part) of the same patient. The histogram percentage of 90% (perc90), histogram percentage of 99% (perc99), and AngScMom (uniformity) rates were significantly higher in the malignant group, whereas the entropy rates were considerably higher in the benign group. The ratios were calculated as nodule area measurements and contralateral nodule-free area measurements.

Comparison between CTTA and radiologist

Two radiologists, who were blinded to the final histopathology of the patients, performed differential diagnoses using the CT images of the cohort. Their ability to detect malignant cases compared with CTTA model-based diagnosis was measured. The CTTA model demonstrated a sensitivity of 81.4% and specificity of 37.8%. In comparison, the first radiologist achieved a sensitivity of 51.2% and a specificity of 29.7%, whereas the second radiologist achieved a sensitivity of 55.8% and a specificity of 37.8%. Additionally, the CTTA model achieved the highest accuracy at 61.3%, followed by the first radiologist at 41.3% and second radiologist at 47.5%. On average, the CTTA model performed significantly better than the two radiologists, especially with regard to sensitivity.

DISCUSSION

Thyroid nodules are prevalent in more than half of the adult patients undergoing thyroid imaging. Research indicates that approximately 7% of these nodules have been identified as malignant (11). In cases where benign nodules do not result in thyroid dysfunction, respond to antithyroid treatment, and do not cause functional disorders due to compression of the surrounding structures, follow-up is typically deemed adequate. However, surgery is generally considered unavoidable action for malignant nodules. Early detection of thyroid nodules is crucial for effective management and minimising unwarranted morbidity.

USG is a key diagnostic modality in the primary assessment of thyroid nodules because of its cost-effectiveness and utility. In addition to USG, CT, magnetic resonance imaging (MRI), and positron emission tomography (PET) are valuable diagnostic modalities. CT is particularly advantageous in diagnosing retrosternal goitres and suspected extracapsular spread in cases of malignancy. CT is a notable modality for identifying incidental thyroid nodules. Variations are discernible in the interpretation of these nodules. In contrast to USG, experts lack

agreement regarding the potential for malignancy associated with the nodule characteristics identified on CT scans.

Texture analysis can offer qualitative and quantitative evaluation by scrutinising the dispersion and interdependence of grey levels within images. The potential heterogeneity of tumour tissue structure may lead to varying outcomes in the texture analysis approach. The subtypic of renal cell carcinoma, differentiation of portal vein thrombus between malignant-benign groups, differentiation of high- and low-grade intraductal papillary mucinous neoplasms of the pancreas, differentiation of intestinal polyps from neoplastic-nonneoplastic, and differentiation of benign-malignant lung nodules have yielded significant results through texture analysis, as reported in the literature (10). Although there is an increasing number of studies on texture analysis, research specifically focussed on texture analysis of thyroid nodules or malignancies is sparse.

To date, numerous research endeavours have been conducted to assess the efficacy of CT imaging in diagnosing thyroid nodules. The evaluation of thyroid nodules was conducted by Li et al. through the utilisation of dual-energy (dual phase) CT images, as reported in their study (12). A notable dissimilarity was observed between benign and malignant thyroid nodules in terms of their iodine concentration, HU values, and adequate atomic numbers (12). Yoon et al. conducted a retrospective analysis of thyroid nodules incidentally detected on neck CT scans and identified characteristics that indicate malignant potential (13). The authors contended that the presence of calcification at the periphery of the nodule, a high ratio of anterior-posterior diameter to transverse diameter (AP/T ratio), and a mean attenuation value measured in HU exceeding 130 were indicative of an elevated likelihood of the nodule Benign malignant. The authors contended that the risk of malignancy in incidental thyroid nodules identified on CT scans, as determined by the same study, was relatively low at 9.4%. Therefore, they concluded that there is no requirement for supplementary assessment with USG without any malignancy-suggestive features. Lee et al. conducted a study on 259 patients, and their findings were consistent with those of Yoon et al. The study found that small nodules with low mean attenuation values and homogeneous characteristics were frequently benign (14). Our study concluded that a significant proportion of patients (69.2%) with calcification on preoperative USG had malignancy. The identification of calcification through CT imaging, coupled with the characterisation of such calcification, the detection of irregularities in the margin of the thyroid nodule, and the observation of a heterogeneous structure within the nodule indicate a higher likelihood of malignancy (12-14). Given this information, as the number of research utilising CTTA models in thyroid nodules continues to rise, it is important to provide supplementary parameters to augment the features acquired from USG to differentiate between benign and malignant nodules.

In this study, texture analysis was conducted using first- and second-degree statistics, and 21 distinct features were

evaluated. Initially, the preoperative USG results, which included the identification of calcification, solid-cystic structure, and echogenicity assessment, were compared with the texture analysis data acquired from the CT section. Our study revealed that nodules with calcification exhibited higher correlation values, indicating a significant pixel correlation with the adjacent tissue. This finding was interpreted as a potential indicator of malignancy because a higher correlation value may suggest a greater likelihood of malignancy. In addition, the predominance of solid or cystic components of the nodule was compared with the data obtained from texture analysis. A statistically significant difference was observed in the mean, kurtosis, and histogram percentage measurements between solid and cystic nodules. Specifically, the measurements of Perc01, Perc10, Perc50, Perc90, and Perc99 showed significant differences. No statistically significant discrepancy was observed between the echogenicity observation assessed through USG and the texture analysis information. Studies have been conducted in the literature on USG-based texture analysis to quantify radiologists' subjective comments regarding thyroid USG examination (15). Jung et al. conducted research to differentiate benign (K-TIRADS 2) and suspicious (K-TIRADS 3, 4, 5) nodules on chest CT by CTTA (16). The model incorporating MPP, kurtosis, and skewness with a medium philtre using the single most extensive cross-section analysis correctly predicted the suspicious nodules with high sensitivity and specificity (84.4% and 81.0%, respectively). In our study, we conducted CT-based texture analysis without computer-assisted filtering programmes and compared the resulting parameters with preoperative USG findings. Due to the lack of comparable conclusions in the existing literature, it is impossible to draw a comparative analysis. Nevertheless, the texture analysis parameters acquired during our study regarding the differentiation of calcification present-absent and solid-cystic are noteworthy (15).

The research's second phase involved comparing postoperative thyroid histopathology and texture analysis data, which yielded no statistically significant differences. The usability of texture analysis data as a diagnostic test was assessed by examining the results of the ROC curve analysis. The findings indicated that the areas under the curve were not statistically significant, concluding that this method is inappropriate for distinguishing between benign and malignant conditions. After conducting a logistic regression analysis, the accuracy rate of the model was determined to be 61.3%. The study revealed that the Perc99 (Histogram percentage-99%) and HU measurements substantially contributed to the model. The data indicate that an increase of 0.006 units in the Perc99 metric is associated with a 1.006-fold reduction in the probability of malignancy. Furthermore, an increase in the HU measurement by 0.023 units led to a 1.024-fold increase in the risk of malignancy. The correlation between the elevation of HU and the heightened probability of malignancy is consistent with previous findings in the literature (12, 13).

In the third stage of the research, a comparison was made between the texture analysis data obtained from the section

extracted from the nodule and the texture analysis data obtained from the section extracted from the nodule-free side, which refers to the relatively intact thyroid tissue. Upon comparing the data of nodule tissue and nodule-free tissue in each patient, it was observed that the malignant group exhibited higher rates of Perc90 (Histogram percent-90%), Perc99 (Histogram percent-99%), and AngScMom (Angular second moment- angular second moment, uniformity). In contrast, the benign group demonstrated a significantly higher entropy value. The measure of uniformity, also known as the angular second moment, pertains to the evenness of the distribution of intensity levels in an image; on the other hand, entropy characterises the degree of randomness and irregularity in pixel density. In our study, the observed high degree of uniformity within the malignant group and elevated entropy within the benign group may indicate that benign nodules exhibit more significant heterogeneity than malignant nodules compared with normal thyroid tissue. However, it is advisable to conduct a comprehensive assessment of the texture analysis information rather than relying solely on individual interpretations. A study similar to the one led by Liu et al. involved CT-based texture analysis and a support vector machine (SVM) to examine thyroid nodules. The researchers evaluated the programme's efficacy following filtering through a computer-assisted programme to enhance the sensitivity and specificity of the acquired data (17). As a result, it was found that in multiple punctate calcifications in the nodule, the mean intensity, standard deviation, and entropy increased while the uniformity decreased. The study also revealed that the accuracy of thyroid cancer prediction was 0.8673 after utilising a computer-aided programme to philtre texture analysis data. However, the accuracy rate of our model was low (0.613) in differentiating benign-malignant nodules in various patients; this could be attributed to the lack of use of a computer-aided filtering programme in the study. Peng et al. conducted a study that extracted first-order statistical features and used SVM to identify normal thyroid tissues and nodules based on CT images (18). The study revealed notable dissimilarities in entropy, uniformity, standard deviation, and skewness measurements in the nodule area compared with healthy thyroid tissue, which can be attributed to the heterogeneous composition of the nodule tissue. Our study differs from Peng et al. 's study in that it involves the use of images that depict the thyroid nodule, followed by the application of a texture analysis method after manual marking and aimed to investigate potential disparities in the differentiation of benign and malignant nodules using texture analysis techniques, as opposed to the system that distinguishes the existing nodule from the surrounding normal thyroid tissue.

To the best of our knowledge, although there are comparative analyses between the texture analysis of USG images and the subjective analysis of radiologists (19, 20), no study has been conducted to compare the classification of thyroid nodules using CT texture analysis and subjective assessment by radiologists. In our study, compared with the first and second radiologists, the CTTA model was superior at differentiating between benign and malignant thyroid nodules. CTTA will not

replace radiologists in the upcoming years. However, medical experts can still benefit from CTTA-based solutions to extend their understanding of thyroid nodules in their routine practise.

This study is subject to certain limitations. First, radiologists must outline the ROIs on the CT slices manually. Our prospective efforts include implementing automated segmentation techniques for the thyroid region of interest (ROI) to enhance operational effectiveness. Other limitations include the small number of patients and computer-assisted filtering programmes not being used to analyse texture analysis data. Evaluating CT sections from more patients is necessary to standardise the current method. Other limitations of the study are that the study was retrospective, not all features were reported on USG (54 patients (67.5%) who were not assessed for calcification on USG, 26 patients (32.5%) who were not evaluated for echogenicity, and 22 patients (27.5%) whose solid-cystic distinction was not considered), and the same radiologist did not evaluate USG.

CONCLUSION

When evaluating thyroid nodules, quantitative data can be obtained via texture analysis. Although texture analysis cannot substitute for USG, it produces promising results in providing further information in thyroid nodule assessment. Other multicenter prospective trials, including larger cohorts of patients, should corroborate these findings.

Ethics Committee Approval: This study was approved by the Ethics Committee of the Marmara University (Date: 18.06.2021, No: 09.2021.396).

Informed Consent: Due to the retrospective design of the study, informed consent was not taken.

Peer Review: Externally peer-reviewed.

Author Contributions: Conception/Design of Study- Ö.T.K., S.İ.; Data Acquisition- S.İ., B.K.; Data Analysis/Interpretation- Ö.T.K., S.İ.; Drafting Manuscript- Ö.T.K., B.K.; Critical Revision of Manuscript- S.İ., A.C.Y.; Final Approval and Accountability- A.C.Y., S.İ.; Material or Technical Support – B.K., A.C.Y.; Supervision- A.C.Y.

Conflict of Interest: The authors have no conflict of interest to declare.

Financial Disclosure: The authors declared that this study has received no financial support.

REFERENCES

1. Jemal A, Siegel R, Ward E, Hao Y, Xu J, Murray T, et al. Cancer statistics, 2008. CA 2008;58(2):71-96.
2. Hundahl SA, Cady B, Cunningham MP, Mazzaferri E, McKee RF, Rosai J, et al. Initial results from a prospective cohort study of 5583 cases of thyroid carcinoma treated in the United States during 1996: an American college of surgeons commission on cancer patient care evaluation study. Cancer 2000;89(1):202-17.
3. Gopinath B, Shanthi N. Computer-aided diagnosis system for classifying benign and malignant thyroid nodules in multi-stained FNAB cytological images. ACPSEM 2013;36:219-30.
4. Kwak JY, Han KH, Yoon JH, Moon HJ, Son EJ, Park SH, et al. Thyroid imaging reporting and data system for US features of nodules: a step in establishing better stratification of cancer risk. Radiology 2011;260(3):892-9.
5. Yoon JH, Kim E-K, Hong SW, Kwak JY, Kim MJ. Sonographic features of the follicular variant of papillary thyroid carcinoma. J Ultrasound Med 2008;27(10):1431-7.
6. Orhan A, Yumuşakhuylu A, GÜNDOĞMUŞ CA, Çağatay O. Ultrasonographic and Cytological Diagnostic Difficulties of Follicular-Variant Papillary Thyroid Carcinoma. Tr-ENT. 2021;31(1):1-5.
7. Moschetta M, Ianora AAS, Testini M, Vacca M, Scardapane A, Angelelli G. Multidetector computed tomography in the preoperative evaluation of retrosternal goiters: a useful procedure for patients for whom magnetic resonance imaging is contraindicated. Thyroid 2010;20(2):181-7.
8. Ishigaki S, Shimamoto K, Satake H, Sawaki A, Itoh S, Ikeda M, et al. Multi-slice CT of thyroid nodules: comparison with ultrasonography. Radiation Med 2004;22(5):346-53.
9. Bin Saeedan M, Aljohani IM, Khushaim AO, Bukhari SQ, Elnaas ST. Thyroid computed tomography imaging: pictorial review of variable pathologies. Insights imaging 2016;7(4):601-17.
10. Lubner MG, Smith AD, Sandrasegaran K, Sahani DV, Pickhardt PJ. CT texture analysis: definitions, applications, biologic correlates, and challenges. Radiographics 2017;37(5):1483-503.
11. Hegedüs L. The thyroid nodule. NEJM 2004;351(17):1764-71.
12. Li M, Zheng X, Li J, Yang Y, Lu C, Xu H, et al. Dual-energy computed tomography imaging of thyroid nodule specimens: comparison with pathologic findings. Invest Radiol 2012;47(1):58-64.
13. Yoon DY, Chang SK, Choi CS, Yun EJ, Seo YL, Nam ES, et al. The prevalence and significance of incidental thyroid nodules identified on computed tomography. JCAT 2008;32(5):810-5.
14. Lee C, Chalmers B, Treister D, Adhya S, Godwin B, Ji L, et al. Thyroid lesions visualized on CT: sonographic and pathologic correlation. Acad Radiol 2015;22(2):203-9.
15. Sollini M, Cozzi L, Chiti A, Kirienko M. Texture analysis and machine learning to characterize suspected thyroid nodules and differentiated thyroid cancer: Where do we stand? Eur J Radiol 2018;99:1-8.
16. Jo JI, Im Kim J, Ryu JK, Lee HN. Incidental Thyroid Nodule on Chest Computed Tomography: Application of Computed Tomography Texture Analysis in Prediction of Ultrasound Classification. JCAT 2022;46(3):480-6.
17. Liu C, Chen S, Yang Y, Shao D, Peng W, Wang Y, et al. The value of the computer-aided diagnosis system for thyroid lesions based on computed tomography images. QIMS 2019;9(4):642.
18. Peng W, Liu C, Xia S, Shao D, Chen Y, Liu R, et al. Thyroid nodule recognition in computed tomography using first order statistics. Biomed Eng Online 2017;16:1-14.
19. Nam SJ, Yoo J, Lee HS, Kim E-K, Moon HJ, Yoon JH, et al. Quantitative evaluation for differentiating malignant and benign thyroid nodules using histogram analysis of grayscale sonograms. J Med Ultrasound 2016;35(4):775-82.

20. Chang Y, Paul AK, Kim N, Baek JH, Choi YJ, Ha EJ, et al. Computer-aided diagnosis for classifying benign versus malignant thyroid nodules based on ultrasound images: a comparison with radiologist-based assessments. Med Phys 2016;43(1):554-67.